NANO LETTERS

Letter

pubs.acs.org/NanoLett

On-Surface Engineering of a Magnetic Organometallic Nanowire

Maider Ormaza,[*,†] Roberto Robles,[‡] Nicolas Bachellier,[†] Paula Abufager,[‡,§] Nicolás Lorente,[‡,∥,⊥] and Laurent Limot[†]

[†]IPCMS, CNRS UMR 7504, Université de Strasbourg, 67034 Strasbourg, France

[‡]ICN2 - Institut Català de Nanociéncia i Nanotecnologia, Campus UAB, 08193 Bellaterra (Barcelona), Spain

[§]Instituto de Física de Rosario, Consejo Nacional de Investigaciones Científicas y Técnicas (CONICET) and Universidad Nacional de Rosario, Avenida Pellegrini 250 (2000) Rosario, Argentina

[∥]Centro de Física de Materiales CFM/MPC (CSIC-UPV/EHU), Paseo Manuel de Lardizabal 5, 20018 Donostia-San Sebastián, Spain

[⊥]Donostia International Physics Center (DIPC), Paseo Manuel de Lardizabal 4, 20018 Donostia-San Sebastián, Spain

Supporting Information

ABSTRACT: The manipulation of the molecular spin state by atom doping is an attractive strategy to confer desirable magnetic properties to molecules. Here, we present the formation of novel magnetic metallocenes by following this approach. In particular, two different on-surface procedures to build isolated and layer-integrated Co-ferrocene (CoFc) molecules on a metallic substrate via atomic manipulation and atom deposition are shown. The structure as well as the electronic properties of the so-formed molecule are investigated combining scanning tunneling microscopy and spectroscopy with density functional theory calculations. It is found that unlike single ferrocene a CoFc molecule possesses a magnetic moment as revealed by the Kondo effect. These results correspond to the first controlled procedure toward the development of tailored metallocene-based nanowires with a desired chemical composition, which are predicted to be promising materials for molecular spintronics.

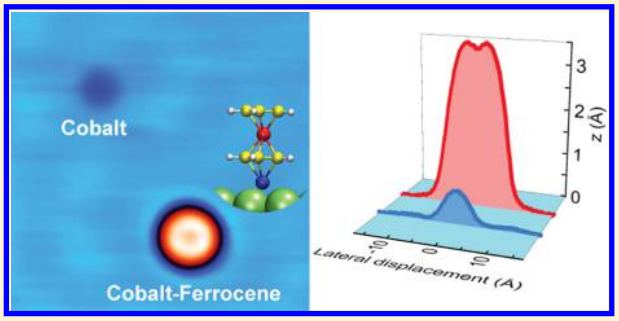

KEYWORDS: *Ferrocene, spin doping, Kondo effect, tip-assisted manipulation, scanning tunneling microscopy/spectroscopy, density functional theory*

The ability to manipulate the magnetic properties and the spin-polarized current through single molecules is at the basis of molecular spintronics.[1−4] The spin and the electronic structure of the molecule near the Fermi level critically influence the spin-polarization of the current,[5,6] opening up the tantalizing prospect of tuning the spin polarization through a custom-made chemistry of the molecule and an accurate choice of the electrode material. Within this context, the investigation of single molecules with built-in magnetic moments that are coupled to ferromagnetic, or more generally, to metallic electrodes represents a model playground for exploring novel spintronic concepts.[7]

Many experimental investigations have reported on the possibility of manipulating the molecular spin by metallizing or altering the chemical environment of porphyrin-based[8−11] or phthalocyanine-based[12−18] molecules adsorbed on metallic surfaces or of cobalt complexes coupled to metallic electrodes.[19,20] Experimental studies of this kind on single metallocenes (MCp_2 where Cp = C_5H_5 and M = Fe, Co, Ni, and so forth) remain instead limited, despite numerous studies have predicted that metallocene-based nanowires[21−29] (M−Cp−M−Cp−...) could produce highly spin-polarized charge carriers. The efficiency of this process is influenced by the metallic constituents of the nanowires,[24,29] the wire length,[26] and by the geometry of the metal-wire contact.[25] Progress in this area is hampered by the difficulty encountered in synthesizing these molecules in the correct molecular-device environment. The demand for elaborating a prototypical system with atomic-scale control is therefore strong.

We present here a general method for modifying the structure and magnetic moment of a metallocene molecule by coupling it to a single atom. The method is exemplified by using a ferrocene molecule ($FeCp_2$, noted Fc hereafter) and a cobalt atom adsorbed onto a copper surface. Ferrocene represents the most commonly considered metallocene as its anchoring to surfaces has been studied for years[30] in view of applications ranging from charge storage[31] to transistors.[32] By manipulating ferrocene and cobalt with the tip of a low-temperature scanning tunneling microscope (STM) and forcing them to interact with each other, we show that we can produce a small nanowire consisting of Co−Cp−Fe−Cp (noted CoFc hereafter; see Figure 1e). The upstanding geometry obtained for CoFc on the surface is ideal for elaborating a single-

Received: October 21, 2015
Revised: December 8, 2015
Published: December 9, 2015

DOI: 10.1021/acs.nanolett.5b04280
Nano Lett. 2016, 16, 588−593

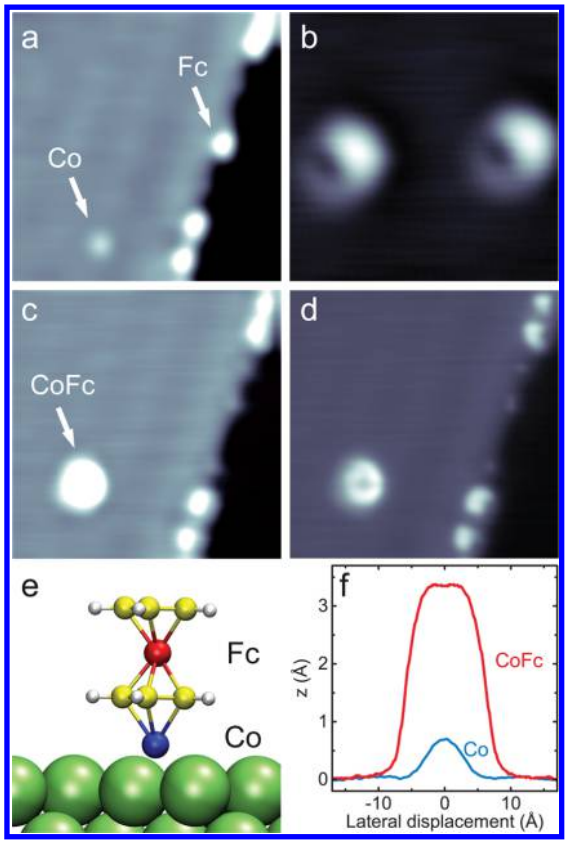

Figure 1. Building process of an isolated CoFc: (a) a Fc molecule at a step edge is picked up with the tip (image acquired with a tunneling bias: − 1 V, current: 20 pA; image size: 7 × 7 nm^2), (b) the presence of Fc at the tip apex is asserted by imaging Co atoms (−50 mV, 20 pA, 2.7 × 2.7 nm^2), which then exhibit a molecular pattern, (c) Fc is deposited on top of a Co atom by a tip-atom contact (−1 V, 20 pA, 7 × 7 nm^2). (d) Same image as panel (c) but with a Laplacian filter applied in order to enhance the intramolecular contrast. (e) Chemical structure of CoFc; white, yellow, and red balls represent H, C, and Fe atoms of the Fc molecule respectively, and green balls represent the Cu atoms of the Cu(111) surface. (f) Line profiles of isolated Co and CoFc on Cu(111).

molecule device, for example, by a subsequent connection of the nanowire to a top electrode. To generalize the process to a collection of molecules, we also show that CoFc can be produced through a spontaneous on-surface reaction of cobalt atoms with a molecular layer of ferrocene. Through a combined STM and density functional theory (DFT) study, we then show that unlike Fc,[25] CoFc exhibits a magnetic moment. These results are a substantial advance upon existing studies devoted to metallocene nanowires as to date the production and magnetic characterization of these systems are restrained to the gas-phase.[33,34] Our findings can be easily generalized to other metallocenes and to ferromagnetic surfaces.

The measurements were performed with a STM working in ultrahigh vacuum (UHV) at 4.4 K using a pristine Cu(111) surface (see experimental details in the Supporting Information). Ferrocene molecules were sublimated in UHV onto the surface held at a temperature below 100 K. A submonolayer coverage of Fc molecules gives rise to a molecular decoration of the surface steps, as shown by the 0.2 monolayer coverage in Figure 1a. According to the Cp ring-like shape observed in the STM images, ferrocenes are adsorbed individually and vertically at the step edges, that is, with the molecular axis perpendicular to the surface. Subsequent deposition of Co atoms at 4.4 K leads to a surface in which Co atoms are placed on the terraces and Fc molecules at the step edges (Figure 1a).

The STM tip is then used as a tool to engineer isolated single CoFc molecules, following the procedure displayed in Figure 1a−d. The first step toward the formation of a novel CoFc molecule consists in positioning the tip on top of a single Fc molecule and approaching it while keeping the bias constant (−150 mV) until an abrupt drop is observed in the current (not shown). This jump in the current indicates that the molecule has been detached from the surface and is now attached to the tip,[35] as revealed by the after-images shown in Figure 1c,d. In Figure 1b, a closer view of the Co atom imaged with the Fc-terminated tip is shown. The Co atom, which is round when imaged with a metallic tip as in Figure 1a, exhibits now a molecular pattern that corresponds to a reverse image of the apex.[36−38] The ring-shape tip apex corresponds to a Cp ring of a tilted Fc molecule.[39] Placing this molecular tip on top of the Co atom and proceeding the same way, that is, decreasing the tip−sample distance until a certain threshold value, we are able to release the molecule from the tip. Figure 1c shows how the targeted Fc molecule has disappeared from the step edge and that a new stable molecule, made up of Co−Cp−Fe−Cp (see sketch in Figure 1e), has been created in the place where the isolated Co atom was. The new CoFc molecule presents a ring-shaped feature as shown in Figure 1d. The corresponding apparent height profiles of an isolated Co atom and a CoFc molecule, 0.7 ± 0.1 and 3.4 ± 0.2 Å respectively, are displayed in Figure 1f. This molecular building process is fully reproducible.

In order to experimentally confirm that a new molecule is formed, we move the whole CoFc molecule by trapping it using a tip-induced local potential. The STM image of Figure 2a reveals that when changing the tunneling current from 50 pA to 2 nA (at a constant bias of −30 mV) the CoFc follows the tip movement and the image is then acquired by dragging the CoFc across the Cu(111) surface. Atomic resolution of Cu(111) is obtained when CoFc is dragged, as was evidenced for a Co atom trapped under the STM tip and rastered over the surface.[40] As expected, a Cu−Cu distance of 2.5 Å is found. Once the current is set back to 50 pA the molecule is released. This supports the idea that CoFc behaves as a unique entity, that is, the interaction between Co and Fc is strong enough to create a new molecular species. Isolated CoFc is coupled stronger to the Cu surface compared to Fc, because no isolated Fc can be found on Cu terraces.

Indeed, DFT calculations show that the role of the surface is to passivate the otherwise reactive CoFc species. Ab initio calculations have been performed within the DFT as implemented in the VASP code.[41,42] We have used the generalized gradient approximation for the exchange and correlation functional[43] and the DFT+D2 method proposed by Grimme[44] to treat the missing van der Waals interactions (more details can be found in the Supporting Information).

These calculations show that due to the location of dangling bonds at the Co edge, the molecule prefers to bind by the Co atom to the surface, although the binding by the Cp ring of the Fc unit is also stable. The Co−Fc bond can be severed by transferring 1.86 eV to the molecule when it is adsorbed by the Co atom, and 1.10 eV when adsorbed by the Fc end. Therefore, the surface stabilizes the CoFc, which results to be a molecular unit with a radical character, via passivation of the Co atom. In fact, the molecule is found to be more stable when an extra Cp

DOI: 10.1021/acs.nanolett.5b04280
Nano Lett. 2016, 16, 588−593

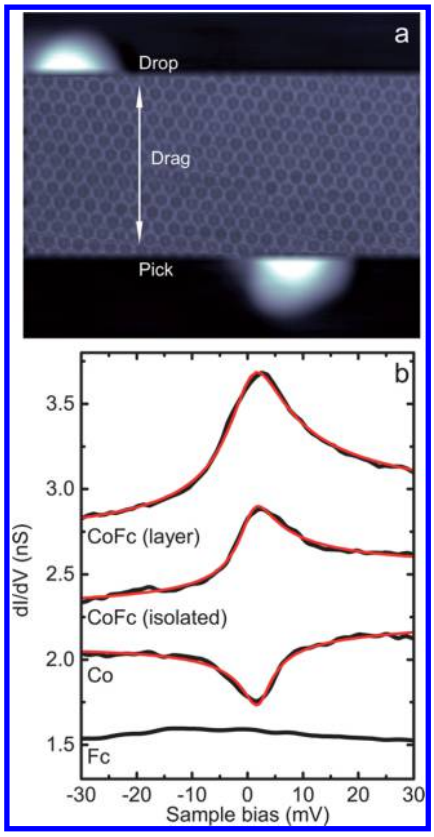

Figure 2. (a) CoFc dragging on Cu(111) (image size: 6.5 × 5.2 nm^2). The dragging parameters are 2 nA and −30 mV. (b) dI/dV spectra including Frota-Fano fits (solid red line) of isolated Co, Fc, CoFc, and layer-integrated CoFc. The curves are shifted by 0, 0.3, 0.5, and −6.8 nS, respectively. The feedback loop was opened at −0.03 V and 0.05 nA for all spectra except for the layer-integrated CoFc where the feedback was opened at −0.05 V and 0.5 nA.

is added to form CpCoFc.[45] Table 1 summarizes the computed chemisorption properties of a Co atom on a face-center cubic

Table 1. Adsorption Properties of a Co atom, a Co Atom Bound to a Fc Molecule and a Co Atom Underneath One of the Eight Fc Molecules for a Compact Arrangement[a]

	d [Co−Cu] (Å)	μ [Co] (μ_B)	μ [Fe] (μ_B)	ΔN [Co] (e^-)	E_B (eV)
Co	1.73	2.09		−0.16	−3.32
CoFc (isolated)	1.70	1.33	0.12	−0.34	−4.04
CoFc (layer)	1.75	1.44	0.11	−0.34	−4.21

[a]The first column is the vertical distance of the Co atom to the topmost layer d in Å; the second and third ones are the magnetic moments μ in Bohr magnetons (μ_B) of Co and Fe atoms, respectively; the fourth column is the change in the number of electrons of the Co atom; and the last one corresponds to the binding energy of Co in the different systems.

(fcc) site of the Cu(111) surface, and their evolution when a Fc molecule is placed on top of the Co atom. The Co atom yields more electrons when the Fc molecule is placed on top describing a stronger binding of the Co atom. However, the adsorption geometry of the Co atom is basically unaltered.

The dI/dV spectra near the Fermi energy for isolated Co, Fc, and CoFc, recorded with a lock-in amplifier (1 mV rms, 782 Hz), are shown in Figure 2b. While no spectroscopic feature is observed for Fc around zero bias, a peak is detected at the Fermi level for CoFc. Its narrow line shape suggests that it corresponds to a Kondo resonance, as evidenced for other organometallic molecules.[15,17] The Kondo resonances exhibited by Co and CoFc on Cu(111) are fitted using a Frota-Fano function (see Supporting Information),[46,47] as shown in Figure 2b. The line width of CoFc yields a Kondo temperature of T_K = 33 ± 7 K, which is higher than that of an isolated Co atom where T_K = 19 ± 5 K. To confirm the resonance assignment to a Kondo effect, we also compared the spectra of Co and of CoFc on the Cu(100) surface as the Kondo resonance is known to depend on the hybridization of cobalt with the surface.[48] As expected,[49,50] on Cu(100) the Kondo temperature increases yielding, respectively, 35 ± 5 K for Co and 114 ± 7 K for CoFc (see Figure S1 in the Supporting Information). The line shape evolution from a resonance to a dip seen in Figure 2b is quantified by the difference in the Fano fitting parameter found for CoFc (q = 7 ± 3) compared to Co (q = 0.10 ± 0.05). This underlines that the orbitals and tunneling paths involved in the Kondo physics are different in the two systems.[51] The increased value of q for CoFc is in particular consistent with the higher corrugation of CoFc compared to a Co atom on Cu(111) that places the tip further away from the surface thereby weakening the direct tunneling into the electron continuum of copper.[52]

The presence of a Kondo effect indicates that CoFc has a magnetic moment. DFT calculations that consider the Cu(111) surface show in particular that the magnetic moment of the Co atom is reduced when bound to Fc due to the increase of occupation of the d-shell. In the molecule, the occupied peaks for the majority density of states (DOS) of Co shift to higher energies compared to an isolated Co, hybridizing with states coming from Fc (Figure 3). The Fc molecule becomes polarized in spin and the majority spin DOS splits to hybridize with the Co levels. Similar changes occur for the minority spin. The transformation of the DOS due to the Co−Fc interaction, reveals the hybridization of the electronic structure forming a molecular unit and the partial depletion of Co levels leading to a reduction of the magnetic moment. In the CoFc molecule, the computed magnetic moment of the Co atom is in fact 1.33 μ_B (see Table 1), which is much higher than the magnetic moment of Fe in the same molecule (0.12 μ_B) or the Cp rings (0.02 μ_B). The magnetic moment of Co on Cu(111) is in contrast 2.09 μ_B, which shows that after the formation of CoFc, the Co atom undergoes a transition from $S \approx 1$ to $S \approx 1/2$ revealing the above changes in electronic structure. This corresponds to a charge transfer of 0.43e^- from the CoFc molecule to the surface, compared to the 0.16e^- for the isolated Co atom. Therefore, the Kondo effect of CoFc and of isolated Co are different, which is in agreement with the measured spectral signatures of the Kondo physics. There is a ferromagnetic (FM) coupling between the Fe and Co atoms of CoFc, which is also apparent in the spin density of the molecule, shown in Figure 3b; the Co−Fe hybridization leads to peaks of the Co atom that coincide in energy with peaks of the Fe atom (Figure 3a). Gas phase calculations of CoFc show that the FM solution is 98 meV more stable than the antiferromagnetic (broken symmetry) one. The magnetic moment of CoFc is mainly carried by spin-polarized molecular orbitals (MOs) which are linear combinations of d_{xz} and d_{yz} orbitals of Co and of Fe with a contribution from the p_z-orbitals of the Cp rings. These MOs in which the major weight is on the Co atom are responsible of the observed Kondo effect.

DOI: 10.1021/acs.nanolett.5b04280
Nano Lett. 2016, 16, 588−593

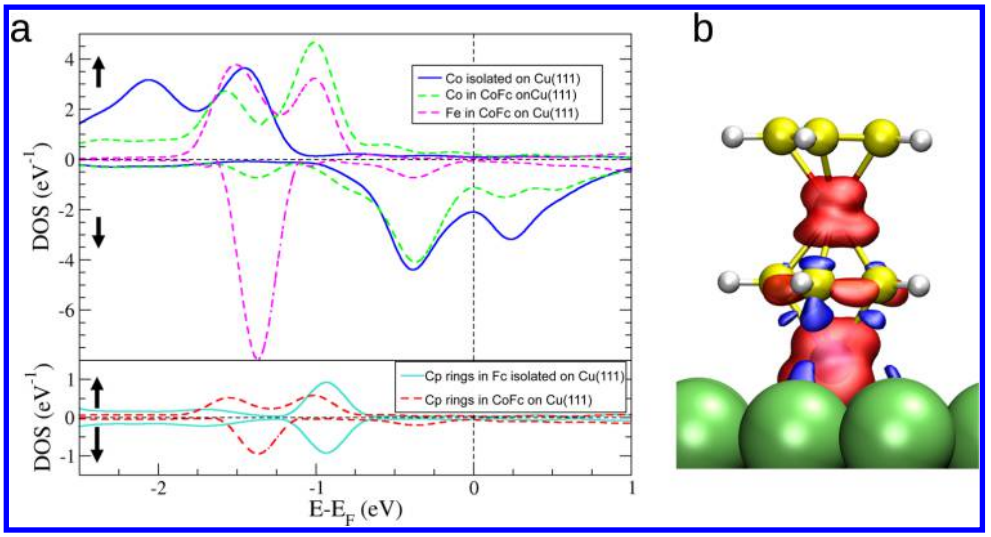

Figure 3. (a) Calculated DOS projected on different atoms of the CoFc molecule (up arrow, majority DOS; down arrow, minority DOS). The dashed lines correspond to the DOS projected onto Co (green), Fe (magenta), and Cp rings (red) when they are part of the new CoFc molecule.The solid lines show the DOS for Co in the absence of Fc (that is, isolated Co) and for Cp rings in the absence of Co (that is, isolated Fc). (b) Spin density for a CoFc molecule at the Fermi level (majority spin, red; minority spin, blue).

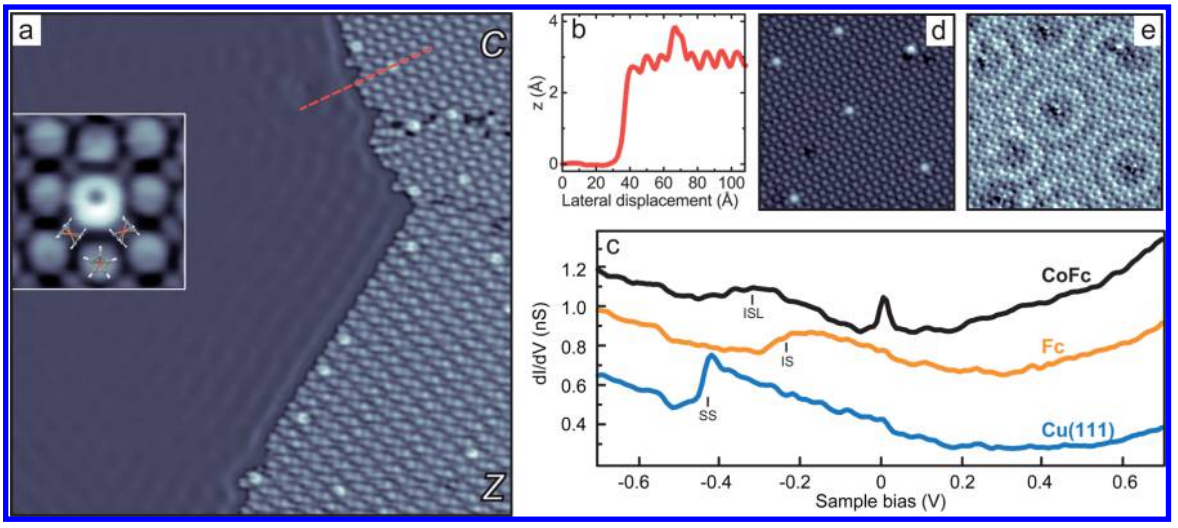

Figure 4. (a) Self-assembly of Fc on Cu(111) (−0.05 V, 0.5 nA, 35 × 35 nm^2). The compact and zigzag arrangements are denoted C and Z, respectively. The bright spots reveal the presence of Co on the molecular layer. Inset: Close up view of the CoFc integrated in the compact configuration. A Fc model structure is superimposed on the image to highlight the adsorption geometry of the ferrocene layer. Note that the Co deposition in panel (a) was done at 77 K, as a consequence the Co atoms on copper have diffused to the step edges. (b) Line profile along the red dashed line shown in (a). (c) dI/dV spectra of Cu(111), Fc, and CoFc. The curves are shifted by 0, 0.3, and 0.5 nS, respectively (feedback loop opened at −1 V and 0.5 nA). (d) CoFc image and (e) corresponding constant-current dI/dV map (−0.1 V, 0.5 nA, 20 × 20 nm^2).

Contributions of Cp rings to this effect are minor due to their negligible magnetic moment.

A different procedure to form the same CoFc molecule is found when increasing the amount of deposited molecules on the surface and sublimating Co atoms afterward. A Co coverage above 0.35 ML starts degrading the ferrocene layer, thus, we will limit to a low coverage regime. Figure 4a shows how a molecular coverage up to 0.6 ML gives rise to densely packed two-dimensional Fc islands. It has been recently shown that Fc molecules physisorb on Cu(111) following two different possible ways of assembly: compact and zigzag.[39] Both arrangements, which can be observed in Figure 4a, consist of a combination of vertical and horizontal molecules, as partially sketched for the compact configuration in the inset. This STM image also shows the surface appearance after exposing it to a small amount of Co atoms (0.05 ML). Among both ferrocene configurations, there is no significant difference regarding the adsorption probability and behavior of the Co atoms. Hence, in the following we will only focus on the compact arrangement.

Adsorbed CoFc molecules appear as bright protrusions in the molecular layer with an apparent height of (0.7 ± 0.1) Å with respect to vertical Fc molecules and (3.7 ± 0.2) Å compared to Cu(111), as deduced from the line profile along the dashed line displayed in Figure 4b. After a careful inspection of the surface, it can be unambiguously concluded that Co atoms are exclusively adsorbed at the sites of vertically oriented ferrocenes. A closer view into the molecular layer in the inset of Figure 4a shows that a novel molecule is formed upon Co adsorption, which appears as a ring with a higher intensity in one of the sides. To determine the adsorption of Co in relation

DOI: 10.1021/acs.nanolett.5b04280
Nano Lett. 2016, 16, 588−593

with the vertical ferrocene, DFT calculations were performed. From total-energy calculations, we conclude that Co atoms prefer to be on an fcc position with respect to the Cu substrate and below Fc, that is, in direct contact with the Cu(111) surface as shown in Figure 5b,c. This conformation is 3 eV more stable than the one with Co on top.

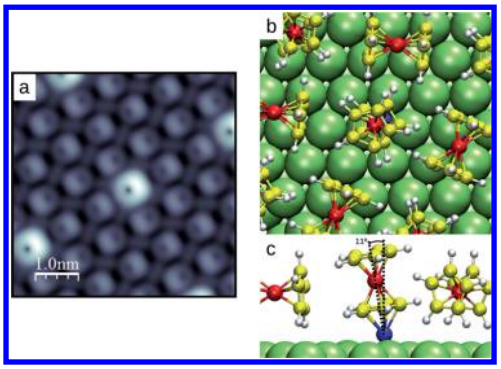

Figure 5. (a) Simulated STM image integrating the local density of states 1 eV above the Fermi energy. The unit cell of the calculation contains a single Co atom per 12 vertically standing Fc molecules. (b,c) Top- and side-view scheme of the compact arrangement with a single Co atom giving rise to a single CoFc molecule in the unit cell. For clarity, only molecules in the middle row of the top view are shown in the side view.

The simulated STM topographic image in Figure 5a, obtained by applying the Tersoff and Hamann theory[53,54] using the method described by Bocquet et al.,[55] shows how a compact molecular layer would look like if we had several CoFc molecules integrated in the ferrocene layer. The ringlike brightest protrusions correspond to CoFc and the dimmer ones to Fc. Horizontal molecules are observed as rodlike features between the vertical ones. The striking agreement between simulated and experimental STM images of the CoFc allows assigning the bright ring-like shape in the images to the top Cp ring of the CoFc molecule. This ring is moreover tilted approximately by 11° with respect to the surface normal (Figure 5c) due to the packing of the molecules.[39] Note that if the Co atom were on top the Fc molecule, according to simulated images (not shown here) no ringlike shape would be observed in the STM images.

To see whether there is any difference between the isolated and the layer-integrated CoFc, the electronic properties of the later one have also been investigated. The dI/dV spectra of Cu(111), Fc, and CoFc are displayed in Figure 4c. The onset of the Shockley surface state (noted SS in Figure 4c) of Cu(111) can be easily identified at −0.44 eV; for the physisorbed ferrocene layer, this state is transformed into an interface state (noted IS) with an onset around −0.26 eV.[56] In the image and associated dI/dV map of Figure 4d,e, the scattering of the interface state of the CoFc is shown, revealing a different coupling of CoFc and Fc with the substrate. In fact, in the dI/dV spectrum of CoFc, a broad resonance is observed around −0.35 V, which corresponds to a localization of the interface state (noted ISL).[52,57−59] More noticeable is the narrow peak detected near zero bias, which as in the previous case can be referred to the Kondo effect presented by CoFc. The resonance is again fitted using a Frota-Fano function as shown in Figure 2b, from which we obtain $T_K = 38 \pm 6$ K and $q = 6 \pm 3$. Compared to the results obtained for the isolated CoFc, we can conclude that both molecules, isolated and layer-integrated, present an experimentally indistinguishable electronic and magnetic behavior.

The computed adsorption properties, Table 1, also show a small variation when going from the isolated molecule to the monolayer. The Co atom stabilizes more the system for the monolayer by a small 5% change in the binding energy and, as a consequence, the Co atom approaches the Fc molecule and separates 0.05 Å from the Cu (111) surface. However, both charge transfer and magnetic moments are similar for the isolated and the monolayer case, showing the calculated DOS a negligible downshift of the Co peaks when going into the monolayer case. Hence, DFT results imply that as in the experiment, both isolated and layer-integrated cases present the same electronic and magnetic behavior. This indicates that the coupling of the molecule with the substrate is similar in both cases and that the neighboring ferrocenes around CoFc in the layer do not interact strongly, as to modify its properties. This is in agreement with the reported weak ferrocene−ferrocene interaction in the ferrocene monolayer.[39]

Summarizing, we have demonstrated that it is possible to build new customized ferrocene-based molecules in a controlled way via STM manipulation and that the same molecule is formed spontaneously by atomic doping of the ferrocene layer, highlighting the stability of this molecule. In particular, we have shown that CoFc exhibits a magnetic behavior, as revealed by the observed Kondo resonance. This result can be generalized to other atoms and metallocene molecules, as we have already checked, opening a path to create and study a whole new family of metallocene nanowires coupled to metal electrodes.

■ ASSOCIATED CONTENT

Supporting Information

The Supporting Information is available free of charge on the ACS Publications website at DOI: 10.1021/acs.nanolett.5b04280.

Details of the experimental methods, DFT calculations and Kondo fitting procedure. STM image and STS spectra obtained for CoFc molecules on Cu(100). (PDF)

■ AUTHOR INFORMATION

Corresponding Author

*E-mail: maider.ormaza@ipcms.unistra.fr.

Notes

The authors declare no competing financial interest.

■ ACKNOWLEDGMENTS

We thank B. W. Heinrich and M. V. Rastei for acquiring preliminary data. We also thank M. Vérot, T. Le Bahers, and M.-L. Bocquet for fruitful discussions. R.R. and N.L. acknowledge financial support from Spanish MINECO (Grant MAT2012-38318-C03-02 with joint financing by FEDER Funds from the European Union). P.A. acknowledges financial support from CONICET. ICN2 acknowledges support from the Severo Ochoa Progam (MINECO, Grant SEV-2013-0295). IPCMS acknowledges financial support from the Agence Nationale de la Recherche through Grant ANR-13-BS10-0016, project LabEx NIE and project LabEx CSC.

■ REFERENCES

(1) Xiong, Z. H.; Wu, D.; Vardeny, Z. V.; Shi, J. *Nature* **2004**, *427*, 821−824.

DOI: 10.1021/acs.nanolett.5b04280
Nano Lett. 2016, 16, 588−593

(2) Bogani, L.; Wernsdorfer, W. *Nat. Mater.* **2008**, *7*, 179−186.
(3) Candini, A.; Klyatskaya, S.; Ruben, M.; Wernsdorfer, W.; Affronte, M. *Nano Lett.* **2011**, *11*, 2634−2639.
(4) Urdampilleta, M.; Klyatskaya, S.; Cleuziou, J.-P.; Ruben, M.; Wernsdorfer, W. *Nat. Mater.* **2011**, *10*, 502−506.
(5) Rocha, A. R.; Garcia-suarez, V. M.; Bailey, S. W.; Lambert, C. J.; Ferrer, J.; Sanvito, S. *Nat. Mater.* **2005**, *4*, 335−339.
(6) Iacovita, C.; Rastei, M. V.; Heinrich, B. W.; Brumme, T.; Kortus, J.; Limot, L.; Bucher, J. P. *Phys. Rev. Lett.* **2008**, *101*, 116602.
(7) Sanvito, S. *Chem. Soc. Rev.* **2011**, *40*, 3336−3355.
(8) Gottfried, J. M.; Flechtner, K.; Kretschmann, A.; Lukasczyk, T.; Steinrück, H.-P. *J. Am. Chem. Soc.* **2006**, *128*, 5644−5645.
(9) Iancu, V.; Deshpande, A.; Hla, S.-W. *Phys. Rev. Lett.* **2006**, *97*, 266603.
(10) Tanaka, H.; Ikeda, T.; Takeuchi, M.; Sada, K.; Shinkai, S.; Kawai, T. *ACS Nano* **2011**, *5*, 9575−9582.
(11) Auwarter, W.; Ecija, D.; Klappenberger, F.; Barth, J. *Nat. Chem.* **2015**, *7*, 105−120.
(12) Zhao, A.; Li, Q.; Chen, L.; Xiang, H.; Wang, W.; Pan, S.; Wang, B.; Xiao, X.; Yang, J.; Hou, J. G.; Zhu, Q. *Science* **2005**, *309*, 1542−1544.
(13) Bai, Y.; Buchner, F.; Wendahl, M. T.; Kellner, I.; Bayer, A.; Steinrück, H.-P.; Marbach, H.; Gottfried, J. M. *J. Phys. Chem. C* **2008**, *112*, 6087−6092.
(14) Sperl, A.; Kröger, J.; Berndt, R. *Angew. Chem., Int. Ed.* **2011**, *50*, 5294−5297.
(15) Komeda, T.; Isshiki, H.; Liu, J.; Zhang, Y.-F.; Lorente, N.; Katoh, K.; Breedlove, B. K.; Yamashita, M. *Nat. Commun.* **2011**, *2*, 217.
(16) Lodi Rizzini, A.; Krull, C.; Balashov, T.; Kavich, J. J.; Mugarza, A.; Miedema, P. S.; Thakur, P. K.; Sessi, V.; Klyatskaya, S.; Ruben, M.; Stepanow, S.; Gambardella, P. *Phys. Rev. Lett.* **2011**, *107*, 177205.
(17) Robles, R.; Lorente, N.; Isshiki, H.; Liu, J.; Katoh, K.; Breedlove, B. K.; Yamashita, M.; Komeda, T. *Nano Lett.* **2012**, *12*, 3609−3612.
(18) Krull, C.; Robles, R.; Mugarza, A.; Gambardella, P. *Nat. Mater.* **2013**, *12*, 337.
(19) Parks, J. J.; Champagne, A. R.; Costi, T. A.; Shum, W. W.; Pasupathy, A. N.; Neuscamman, E.; Flores-Torres, S.; Cornaglia, P. S.; Aligia, A. A.; Balseiro, C. A.; Chan, G. K.-L.; Abrua, H. D.; Ralph, D. C. *Science* **2010**, *328*, 1370−1373.
(20) Wagner, S.; Kisslinger, F.; Ballmann, S.; Schramm, F.; Chandrasekar, R.; Bodenstein, T.; Fuhr, O.; Secker, D.; Fink, K.; Ruben, M.; Weber, H. B. *Nat. Nanotechnol.* **2013**, *8*, 575−579.
(21) Liu, R.; Ke, S.-H.; Baranger, H. U.; Yang, W. *Nano Lett.* **2005**, *5*, 1959−1962.
(22) García-Suárez, V. M.; Ferrer, J.; Lambert, C. J. *Phys. Rev. Lett.* **2006**, *96*, 106804.
(23) Liu, R.; Ke, S.-H.; Yang, W.; Baranger, H. U. *J. Chem. Phys.* **2007**, *127*, 141104.
(24) Wang, L.; Cai, Z.; Wang, J.; Lu, J.; Luo, G.; Lai, L.; Zhou, J.; Qin, R.; Gao, Z.; Yu, D.; Li, G.; Mei, W. N.; Sanvito, S. *Nano Lett.* **2008**, *8*, 3640−3644.
(25) Zhou, L.; Yang, S.-W.; Ng, M.-F.; Sullivan, M. B.; Tan; Shen, L. *J. Am. Chem. Soc.* **2008**, *130*, 4023−4027.
(26) Shen, X.; Yi, Z.; Shen, Z.; Zhao, X.; Wu, J.; Hou, S.; Sanvito, S. *Nanotechnology* **2009**, *20*, 385401.
(27) Yi, Z.; Shen, X.; Sun, L.; Shen, Z.; Hou, S.; Sanvito, S. *ACS Nano* **2010**, *4*, 2274−2282.
(28) Yang, J.-F.; Zhou, L.; Han, Q.; Wang, X.-F. *J. Phys. Chem. C* **2012**, *116*, 19996−20001.
(29) Morari, C.; Allmaier, H.; Beiuşeanu, F.; Jurcuţ, T.; Chioncel, L. *Phys. Rev. B: Condens. Matter Mater. Phys.* **2012**, *85*, 085413.
(30) Finklea, H. O. In *Electroanalytical Chemistry*; Bard, A. J., Rubinstein, I., Eds.; Marcel Dekker, Inc.: New York, 1996; Vol. *19*; pp 109−335.
(31) Fabre, B. *Acc. Chem. Res.* **2010**, *43*, 1509−1518.
(32) Itoh, Y.; Kim, B.; Gearba, R. I.; Tremblay, N. J.; Pindak, R.; Matsuo, Y.; Nakamura, E.; Nuckolls, C. *Chem. Mater.* **2011**, *23*, 970−975.
(33) Nagao, S.; Kato, A.; Nakajima, A.; Kaya, K. *J. Am. Chem. Soc.* **2000**, *122*, 4221−4222.
(34) Miyajima, K.; Nakajima, A.; Yabushita, S.; Knickelbein, M. B.; Kaya, K. *J. Am. Chem. Soc.* **2004**, *126*, 13202−13203.
(35) Eigler, D. M.; Schweizer, E. K. *Nature* **1990**, *344*, 524−526.
(36) Schull, G.; Frederiksen, T.; Brandbyge, M.; Berndt, R. *Phys. Rev. Lett.* **2009**, *103*, 206803.
(37) Heinrich, B. W.; Rastei, M. V.; Choi, D.-J.; Frederiksen, T.; Limot, L. *Phys. Rev. Lett.* **2011**, *107*, 246801.
(38) Chiutu, C.; Sweetman, A. M.; Lakin, A. J.; Stannard, A.; Jarvis, S.; Kantorovich, L.; Dunn, J. L.; Moriarty, P. *Phys. Rev. Lett.* **2012**, *108*, 268302.
(39) Ormaza, M.; Abufager, P.; Bachellier, N.; Robles, R.; Verot, M.; Le Bahers, T.; Bocquet, M.-L.; Lorente, N.; Limot, L. *J. Phys. Chem. Lett.* **2015**, *6*, 395.
(40) Stroscio, J. A.; Celotta, R. J. *Science* **2004**, *306*, 242−247.
(41) Kresse, G.; Furthmüller, J. *Comput. Mater. Sci.* **1996**, *6*, 15.
(42) Kresse, G.; Joubert, D. *Phys. Rev. B: Condens. Matter Mater. Phys.* **1999**, *59*, 1758.
(43) Perdew, J. P.; Burke, K.; Ernzerhof, M. *Phys. Rev. Lett.* **1996**, *77*, 3865.
(44) Grimme, S. *J. Comput. Chem.* **2006**, *27*, 1787.
(45) Abufager, P.; Robles, R.; Lorente, N. *J. Phys. Chem. C* **2015**, *119*, 12119−12129.
(46) Frota, H. *Phys. Rev. B: Condens. Matter Mater. Phys.* **1992**, *45*, 1096−1099.
(47) Pruser, H.; Wenderoth, M.; Dargel, P. E.; Weismann, A.; Peters, R.; Pruschke, T.; Ulbrich, R. G. *Nat. Phys.* **2011**, *7*, 203−206.
(48) Choi, D.-J.; Rastei, M. V.; Simon, P.; Limot, L. *Phys. Rev. Lett.* **2012**, *108*, 266803.
(49) Knorr, N.; Schneider, M.; Diekhöner, L.; Wahl, P.; Kern, K. *Phys. Rev. Lett.* **2002**, *88*, 096804.
(50) Wahl, P.; Diekhöner, L.; Schneider, M. A.; Vitali, L.; Wittich, G.; Kern, K. *Phys. Rev. Lett.* **2004**, *93*, 176603.
(51) Huang, P.; Carter, E. A. *Nano Lett.* **2008**, *8*, 1265−1269.
(52) Madhavan, V.; Chen, W.; Jamneala, T.; Crommie, M.; Wingreen, N. *Phys. Rev. B: Condens. Matter Mater. Phys.* **2001**, *64*, 165412.
(53) Tersoff, J.; Hamann, D. R. *Phys. Rev. Lett.* **1983**, *50*, 1998−2001.
(54) Tersoff, J.; Hamann, D. R. *Phys. Rev. B: Condens. Matter Mater. Phys.* **1985**, *31*, 805−813.
(55) Bocquet, M.-L.; Lesnard, H.; Monturet, S.; Lorente, N. In *Computational Methods in Catalysis and Materials Science*; van Santen, R. A., Sautet, P., Eds.; Wiley-VCH: Weinheim, Germany, 2009; pp 199−219.
(56) Heinrich, B. W.; Limot, L.; Rastei, M. V.; Iacovita, C.; Bucher, J. P.; Djimbi, D. M.; Massobrio, C.; Boero, M. *Phys. Rev. Lett.* **2011**, *107*, 216801.
(57) Olsson, F.; Persson, M.; Borisov, A.; Gauyacq, J.-P.; Lagoute, J.; Fölsch, S. *Phys. Rev. Lett.* **2004**, *93*, 206803.
(58) Limot, L.; Pehlke, E.; Kröger, J.; Berndt, R. *Phys. Rev. Lett.* **2005**, *94*, 036805.
(59) Iancu, V.; Braun, K.-F.; Schouteden, K.; Van Haesendonck, C. *Phys. Rev. Lett.* **2014**, *113*, 106102.

DOI: 10.1021/acs.nanolett.5b04280
Nano Lett. 2016, 16, 588−593